Published in final edited form as:
Ultrasound Med Biol. 2008 June ; 34(6): 892–901.

Doppler estimation of reduced coronary flow reserve in mice with pressure overload cardiac hypertrophy

Craig J. Hartley,
Department of Medicine, Section of Cardiovascular Sciences, Baylor College of Medicine and The Methodist Hospital, Houston, TX 77030

Anilkumar K. Reddy,
Department of Medicine, Section of Cardiovascular Sciences, Baylor College of Medicine and The Methodist Hospital, Houston, TX 77030

Sridhar Madala,
Indus Instruments, Houston, TX 77058

Lloyd H. Michael,
Department of Medicine, Section of Cardiovascular Sciences, Baylor College of Medicine and The Methodist Hospital, Houston, TX 77030

Mark L. Entman, and
Department of Medicine, Section of Cardiovascular Sciences, Baylor College of Medicine and The Methodist Hospital, Houston, TX 77030

George E. Taffet
Department of Medicine, Section of Cardiovascular Sciences, Baylor College of Medicine and The Methodist Hospital, Houston, TX 77030

Abstract

Aortic banding produces pressure overload cardiac hypertrophy in mice leading to decompensated heart failure in 4–8 wks, but the effects on coronary blood flow velocity and reserve are unknown. To determine whether coronary flow reserve (CFR) was reduced, we used noninvasive 20 MHz Doppler ultrasound to measure left main coronary flow velocity at baseline (B) and at hyperemia (H) induced by low (1%) and high (2.5%) concentrations of isoflurane gas anesthesia. Ten mice were studied before (Pre) and at 1d, 7d, 14d, and 21d after constricting the aortic arch to 0.4 mm diameter distal to the innominate artery. We also measured cardiac inflow and outflow velocities at the mitral and aortic valves and velocity at the jet distal to the aortic constriction. The pressure drop as estimated by $4V^2$ at the jet was 51 ± 5.1 (mean ± SE) mmHg at 1d increasing progressively to 74 ± 5.2 mmHg at 21d. Aortic and mitral blood velocities were not significantly different after banding (p = NS), but CFR, as estimated by H/B, dropped progressively from 3.2 ± 0.3 before banding to 2.2 ± 0.4, 1.7 ± 0.3, 1.4 ± 0.2, and 1.1 ± 0.1 at 1d, 7d, 14d, and 21d respectively (all $P < 0.01$ vs Pre). There was also a significant and progressive increase the systolic/diastolic velocity ratio (0.17 Pre to 0.92 at 21d, all $P < 0.01$ vs Pre) suggesting a redistribution of perfusion from subendocardium to subepicardium. We show for the first time that CFR, as estimated by the hyperemic response to isoflurane and

Contact Information: Craig J. Hartley, Ph.D., Professor of Medicine (CVS), Baylor College of Medicine, Methodist Hospital, M/S F-602, Houston, TX 77030, Phone: (713) 798-4195, FAX: (713) 796-0015, Email: cjhartley@ieee.org.
Address for reprint requests: Craig J. Hartley, Dept. of Medicine (CVS), Baylor College of Medicine, One Baylor Plaza, Houston, TX 77030 USA.

measured by Doppler ultrasound, can be measured serially in mice and conclude that CFR is virtually eliminated in banded mice after 21 days of remodeling and hypertrophy. These results demonstrate that CFR is reduced in mice as in humans with cardiac disease but before the onset of decompensated heart failure.

Keywords

blood flow; coronary circulation; hypertrophy; ultrasound; ventricular function

INTRODUCTION

Coronary flow is often normal at rest even in the presence of significant coronary lesions, but maximum flow during exercise or stress can be decreased (Gould et al., 1974). Coronary flow reserve (CFR) is defined as the ratio of maximal-hyperemic/baseline-resting flow or velocity and is often used as an index of the functional severity of coronary stenoses seen angiographically (Cole and Hartley, 1977; White et al., 1984). Coronary flow reserve is also reduced in the presence of valvular and other forms of heart and vascular diseases which increase loading conditions and produce cardiac hypertrophy (Fallen et al., 1967; Marcus et al., 1982; Marcus, 1983; Santagata et al., 2005; Neishi et al., 2005; Parrish et al., 1985). The mechanism for this reduction is thought to be caused by increases in resting baseline coronary flow due to increased cardiac work (Marcus et al., 1982; Eberli et al., 1989; Parrish et al., 1985; Bache et al., 1987). Because oxygen delivery and cardiac work are closely related, the magnitude of CFR is similar to that of cardiac reserve (the ratio of maximal/baseline cardiac output) in normal individuals, and both CFR and exercise capacity tend to be reduced by similar amounts in the presence of cardiovascular disease (Rushmer, 1976). It is thought that decompensated heart failure ensues only after cardiac and coronary reserves are exhausted (Rushmer, 1976; Fallen et al., 1967; Vatner and Hittinger, 1993; Hittinger et al., 1989). Now that mice are being used as cardiovascular disease models (Niebauer et al., 1999; Rockman et al., 1993; Brickson et al., 2006; Barrick et al., 2007; Tanaka et al., 1996; Maslov et al., 2007), it is important to determine if the changes in myocardial perfusion and reserve in the face of increased loading conditions are similar in mice, humans, and larger mammals.

We have recently developed a noninvasive method to measure coronary flow velocity in mice using Doppler ultrasound and have shown that isoflurane gas can be used as a convenient coronary vasodilator when the concentration is increased from 1% to 2.5% (Hartley et al., 2007). We used the ratio of hyperemic/baseline (H/B) left main coronary velocity as an index of CFR, and showed that H/B was a function of age and was reduced in 2-year old apolipoprotein-E null ($ApoE^{-/-}$) mice when compared to age-matched controls as shown in Fig. 1. The increased flow velocity at baseline and during hyperemia in the $ApoE^{-/-}$ mice is consistent with the presence of coronary lesions in some of the mice. Others have shown that cardiac functional reserve as measured by exercise capacity is reduced in $ApoE^{-/-}$ mice (Niebauer et al., 1999), and we have shown that $ApoE^{-/-}$ mice have increased aortic and mitral flow velocity and increased heart-weight/body-weight ratio (HW/BW) consistent with volume overload hypertrophy (Hartley et al., 2000). It is unclear whether the observed decrease in H/B in $ApoE^{-/-}$ mice was due to the presence of coronary lesions restricting hyperemic flow or to the increased baseline cardiac work increasing resting flow.

Transverse aortic banding induces pressure overload cardiac hypertrophy in mice and is used to stress normal, old, and genetically altered mice to study cardiac function and remodeling (Rockman et al., 1993; Li et al., 2003; Brickson et al., 2006; Barrick et al., 2007). Banded mice have significantly elevated HW/BW after 1–5 weeks, some show signs of heart failure, and many die within 3 to 5 weeks after banding (Barrick et al., 2007). In dogs with pressure overload

cardiac hypertrophy it has been shown that CFR is reduced and that the subendocardium becomes more seriously underperfused and dysfunctional (Hittinger et al., 1989; Vatner and Hittinger, 1993; Duncker et al., 1998; Hittinger et al., 1995; Bache et al., 1987). We hypothesized that mice would have lower CFR as estimated by H/B after banding but before the development of symptomatic heart failure. We report here results from 10 mice showing that H/B is progressively decreased and essentially eliminated 21 days after transverse aortic banding. We also observed a significant and progressive increase in the systolic component of coronary flow following aortic banding suggesting a redistribution of flow away from the subendocardium.

METHODS

Animal Protocol

This investigation conforms with the *Guide for the Care and Use of Laboratory Animals* published by the US National Institutes of Health (NIH Publication No. 85–23, revised 1996). Ten C57BL/6 mice were studied following a protocol approved by the Institutional Animal Care and Use Committee of Baylor College of Medicine. For noninvasive measurements (including before banding) mice were anesthetized in a closed chamber with 3% isoflurane in oxygen for 2 to 5 minutes until immobile. Each mouse was then removed, weighed, and taped supine to ECG electrodes on a heated procedure board (MousePad, Indus Instruments, Houston, TX, USA) (Hartley et al., 2002) with isoflurane (initially at 2%) supplied by a nose cone connected to an anesthesia machine (Model V-1 with Isoflurane Vaporizer, VetEquip, Pleasanton, CA, USA). The board temperature was maintained at 35–37 °C. Next, a 2 mm diameter 10 MHz Doppler probe was connected to a Doppler Signal Processing Workstation (Model DSPW, Indus Instruments, Houston, TX, USA) to measure aortic outflow and mitral inflow velocities from the cardiac apex. The probe was then positioned at the right sternal border and pointed toward the aortic arch at the location of the band to record peak velocity at the stenotic jet. Then a 20 MHz Doppler probe was connected, and velocities were measured in the right and left common carotid arteries. After these non-coronary measurements were completed the 20 MHz probe was clamped in a micromanipulator (Model MM3-3, World Precision Instruments, Sarasota, FL, USA) also attached to the procedure board for stability as previously described (Hartley et al., 2007). The clamp on the manipulator gimbal was loosened, and the probe tip was placed on the left chest at the level of the cardiac base and pointed horizontally toward the anterior basal surface of the heart to sense blood flow velocity in the ascending aorta or in the left main coronary artery at a 2.5 mm depth setting. If aortic velocity signals were found first, the sample volume depth was reduced. If coronary velocity signals were found first, the sample volume was advanced until aortic signals were found and then moved back into the left main coronary artery. Coronary flow signals were identified on the Doppler spectral display by flow toward the probe peaking in early diastole and then decaying and being minimal during systole. Once the left main coronary flow signal was obtained, the clamp was tightened, and the sample volume position was adjusted using the depth gate and the three-axis verniers on the manipulator to maximize the velocity and signal strength as seen on the spectral display. In this orientation, the sound beam was nearly parallel to the axis of the left main coronary artery and at right angles to flow in the aorta or pulmonary artery. After a stable signal was achieved, a two-second sample of the ECG and the raw quadrature Doppler signals was acquired and stored in a computer file for later analysis (Hartley et al., 2002). Then the isoflurane concentration was reduced to 1% to lower coronary flow to a baseline level (Hartley et al., 2007). After 3–5 minutes or when flow became stable at the low level, the sample volume was readjusted if necessary to maximize velocity and signal strength, and another two-seconds of signals were collected and stored. Then the isoflurane level was increased to 2.5% to increase coronary flow, and when velocity was stabilized and optimized, more signals were stored and isoflurane was again reduced to 1% and allowed to

stabilize. During this procedure, as coronary blood flow was increased and decreased, a total of 10–15 2-second acquisitions were made to ensure that the maximum and minimum values of coronary velocity were recorded.

After the initial control measurements in each mouse, an aortic band was placed using a procedure described in detail previously (Rockman et al., 1993; Li et al., 2003). Briefly, the mouse was intubated and ventilated, and anesthesia was maintained using 1−2% isoflurane in oxygen. The chest was opened midline, the aortic arch was isolated, and a 27 gauge needle was tied to the ~1.0 mm diameter transverse aorta distal to the origin of the innominate artery using 7.0 silk thread. The needle was immediately removed to create a stenosis of approximately 0.4 mm diameter or a reduction in cross-sectional area of ~84%. The chest was then closed, and the animal was allowed to recover. Measurements as described above were repeated at 1 day, 7 days, 14 days, and 21 days after banding. At 21 days the eight surviving animals were killed, and the hearts were removed and weighed. Fig. 2 contains a diagram of the aortic arch (a) showing the position of the band and the locations of some of the Doppler measurement sites. Also included is a photo of the left and right carotid arteries (b) showing relative dilation of the right carotid artery after banding and Doppler signals (c) measured simultaneously from the aortic arch, the left carotid artery, and the right carotid artery in one of the mice 21 days after banding. Fig. 3 shows representative coronary velocity signals from one mouse at baseline and at hyperemic levels before banding and at 1 day and 21 days after banding.

Instrumentation

The Doppler instrumentation consisted of a 2 mm diameter 20 MHz single-element ultrasonic transducer focused at 4 mm and connected to a 20 MHz pulsed Doppler instrument both of which were constructed in our laboratory (Hartley et al., 2002). The Doppler instrument was optimized for use in mice by setting the burst length to 8 cycles (400 ns) and the pulse repetition frequency (PRF) to 125 kHz. These settings allow the measurement of velocities as high as 4.5 m/s at a maximum sample volume depth of 6 mm. For measurements of aortic and mitral velocities from the apical view, a 10 MHz frequency was used at a PRF of 62.5 kHz to provide a maximum depth of 12 mm. For measurements of aortic arch velocity at the band, the PRF was increased to 125 kHz to resolve a maximum velocity of 9 m/s. The in-phase and quadrature audio signals from the pulsed Doppler instrument were connected to the Doppler Signal Processing Workstation for display, recording, and analysis.

Data Analysis

Data (quadrature audio Doppler signals and lead-2 ECG) were sampled at 125 kHz and stored in 2- second files on a personal computer for later analysis. During analysis a fast Fourier transform (FFT) of the Doppler signals was displayed on the workstation, and a semi-automatic program was used to generate the spectral envelope as illustrated in Fig. 3. The waveform was converted to velocity (V) using the Doppler equation: $V = \Delta f\, c/2f_o \cos\theta$, where Δf is the Doppler frequency, c is the speed of sound in blood (~1,570 m/s), f_o is the ultrasonic frequency (10 or 20 MHz), and θ is the angle between the sound beam and the direction of flow (0° for coronary, aortic, mitral, and aortic arch and 45° for the carotid arteries). From the peak spectral velocity waveforms maximum, minimum, and mean velocities were calculated, and from coronary velocity signals systolic and diastolic time-velocity areas were also calculated as shown in Fig. 3. All beats were averaged for the 2-second data interval (12 to 15 cardiac cycles), and heart rate (HR) was calculated from the R-R interval of the ECG. The hyperemic/baseline ratio of coronary flow (H/B) was calculated from the mean velocity at the highest flow attained during the high level of isoflurane (H) divided by the mean velocity at the minimum baseline flow obtained at the low level of isoflurane (B). Data are presented as mean ± SE, and statistical significance is defined as $P \leq 0.05$ using a paired t-test.

RESULTS

Of the 10 mice which were studied, 1 died between day 1 and day 7 and another between day 14 and day 21 leaving 8 mice alive at 21 days. Heart-weight/body-weight ratio (HW/BW) after 21 days was 8.30 ± 0.43 mg/g. Adequate signals were obtained from all live animals at all time points. Although the mean and SE include data from all mice alive at the time, the *P* values from paired t-tests only include mice which were common to the two groups being compared.

Banded model

Table 1 shows a summary of the data from the 10 mice. There were no significant changes in heart rate, aortic velocity, or mitral velocity after banding. However, there was a significant increase in peak aortic arch velocity caused by the stenotic jet at all times after banding. There were also significant changes in right and left common carotid velocities after banding. The peak velocity in the right carotid artery increased while that in the left carotid artery decreased, and a significant reversal appeared during diastole in the right carotid artery velocity signal after banding. The pulsatility index (PI = (max-min)/mean) increased in the right carotid artery and decreased in the left carotid artery. These changes are consistent with previously reported data (Li et al., 2003) and can also be seen in the example waveforms shown in Fig. 2. We use the right/left peak carotid velocity ratio and the jet velocity at the site of the band to confirm the significance of the aortic constriction and its consistency during the duration of the study.

Coronary blood flow velocity

An example of coronary velocity signals in one mouse taken before, 1 day after, and 21 days after aortic banding at low (1%) and high (2.5%) concentrations of isoflurane gas is shown in Fig. 3. In this mouse the hyperemic response to isoflurane is reduced at 1 day and is eliminated after 21 days. It can also be noted that the systolic component of left main coronary velocity which is minimal before banding becomes nearly equal to the diastolic component at 21 days. Table 1 also shows heart rate (HR), mean coronary velocity, and systolic/diastolic ratio (S/D) both at baseline and during coronary hyperemia. The hyperemic/baseline ratios (H/B) for coronary velocity and HR at all time points are summarized in Fig. 4 which shows a progressive and significant reduction in CFR after banding. Fig. 5 shows the systolic/diastolic time-velocity area ratios (S/D) for coronary velocity at baseline and hyperemia and illustrates a progressive and significant increase in baseline and hyperemic S/D after banding.

DISCUSSION

Characteristics of the banded model

We have previously shown that transverse aortic banding in mice produces peripheral vascular adaptations and alterations including differential changes in velocities, waveforms, and diameters of the right and left carotid arteries after 7 days, but that cardiac function as indicated by aortic and mitral velocities is maintained despite a significant increase in HW/BW (Li et al., 2003). We have also shown (Li et al., 2003) that the pressure drop across the aortic stenosis during systole can be estimated from the peak velocity of the jet measured by Doppler ultrasound and using the simplified Bernoulli equation ($\Delta P=4V^2$) (Hatle et al., 1978). The pressure drop during diastole was found to be minimal, and there were no significant changes in mean abdominal aortic velocity after banding suggesting that pressure was sufficient to maintain adequate perfusion distal to the band.

The mouse model of transverse aortic banding has been adopted and used by many groups to generate pressure overload ventricular hypertrophy (Rockman et al., 1993). The reported increase in HW/BW is 16% at 7 days (Li et al., 2003), 38% at 21 days (Hamawaki et al., 1998; Tanaka et al., 1996), and as much as 56% at 35 days (Brickson et al., 2006). Our values

for HW/BW of 8.3 mg/g in the present study correspond to an increase of 44% when compared to controls done previously by our group using similar methods (5.77 mg/g) (Li et al., 2003). Sakata, et al. (1998) found no changes in end-diastolic or end-systolic ventricular diameter or shortening fraction after 3 weeks of aortic banding in normal wild-type mice. Similarly, Barrick, et al. (2007) found that cardiac function as measured by ejection fraction and diameter shortening fraction was maintained after banding in wild-type C57BL/6 mice for up to 4 weeks after which the mice went into decompensated failure as evidenced by ventricular dilation and reduced shortening fraction at 5 weeks with 60% dying within 8 weeks. After 6 weeks of banding Maslov, et al. (2007) found decreases in ejection fraction and increases in end-diastolic volume but with no changes in stroke volume or cardiac output. In a previous study using M-mode echocardiography, our group found a 22% increase in LV posterior wall thickness but no changes in LV end-systolic diameter, end-diastolic diameter, or diameter shortening fraction after 3 weeks of banding (Zhang et al., 2006). Although we did not measure LV dimensions or shortening fraction in the present study, we found no changes in aortic outflow velocity, mitral inflow velocity, or heart rate suggesting that stroke volume and cardiac output were unchanged at 21 days and that the hypertrophy was compensated.

Reduction in coronary flow reserve

In the present report we have shown for the first time in mice that coronary flow velocity and an estimate of coronary flow reserve are progressively and significantly altered during 21 days following transverse aortic banding. Coronary flow reserve (CFR), as estimated by the hyperemic/baseline coronary velocity ratio (H/B) as isoflurane is increased from 1.0% to 2.5%, is virtually absent 21 days after aortic banding. Similar reductions in CFR have been reported in dogs with cardiac hypertrophy induced by aortic banding (Parrish et al., 1985; Hittinger et al., 1989), and in humans with aortic stenosis (Marcus et al., 1982).

It has been shown that patients with aortic stenosis have reduced CFR (Marcus, 1983; Julius et al., 1997). It is thought that the pressure overload cardiac hypertrophy and increased cardiac work produce an increase in baseline coronary flow and a subsequent decrease in CFR (Eberli et al., 1989; Marcus et al., 1982). These patients also have diminished exercise capacity because of decreased cardiac reserve suggesting that coronary reserve and cardiac reserve are closely connected under conditions of pressure overload (Rushmer, 1976). Similar reductions in exercise capacity and myocardial perfusion have been noted in dogs with banded aortas and cardiac hypertrophy (Parrish et al., 1985; Bache et al., 1987). In a myocardial disease model in mice, it has been shown that CFR as assessed by the hyperemic response to adenosine is reduced from 2.4 to 1.4 following induction of experimental coxsackievirus myocarditis (Saraste et al., 2006).

Use of temporal mean versus peak diastolic velocity

In a previous study (Fig. 1), we calculated H/B from peak diastolic coronary velocities rather than mean velocities (Hartley et al., 2007). In that study there were no significant increases in the systolic component of coronary velocity after vasodilation. Although many other investigators calculate CFR from the ratio of peak diastolic velocities in man (Santagata et al., 2005;Saraste et al., 2001) and in mice (Saraste et al., 2006), we chose to use the temporal mean of the spectral peak for this study (Hozumi et al., 1998) because of the significant amount of flow which occurred during systole. If peak diastolic rather than mean velocities were used to calculate H/B, the values would be under-estimated by 1.5% to 14.6% as shown in Table 1.

Estimation of volume flow changes

The data in Table 1 show that the hyperemic coronary velocity is lower at all times after banding than before, but it is unlikely that coronary volume flow would be reduced during hyperemia in the absence of a coronary stenosis. A possible reason for the observed reduction in velocity

is that the diameter of the left coronary artery may increase after banding due to the high systolic pressure as happens in the right carotid artery (Li et al., 2003) as shown in Fig. 2a or due to flow mediated dilation (Guyton and Hartley, 1985) which has been documented in the large coronary arteries of dogs (Hintze and Vatner, 1984). Other groups have reported increases in ascending aortic diameter proximal to the band in mice (Barrick et al., 2007), and in the present study we noticed that it was easier to obtain Doppler signals from the coronary artery after banding than before. Assuming that there was an increase in left main coronary diameter after banding, it would be necessary to correct coronary velocity to reflect changes in coronary volume flow. However, to our knowledge there are no accurate and noninvasive methods to measure the diameter of the left main coronary artery of a mouse to establish the time course of the dilation (if any).

We have shown in normal mice (Fig. 1) that peak diastolic coronary velocity (PDV) is similar in mice ranging in age from 6 weeks to 2 years (Hartley et al., 2007). Eberli et al. (1989) found in patients that hyperemic coronary volume flow induced by dipyridamole was similar in controls, in patients with aortic stenosis, and in patients following aortic valve repair, but that baseline flows were different. Therefore, we made the assumption that there was at least no decrease in hyperemic coronary volume flow during diastole after banding and normalized both the baseline and hyperemic velocity signals to hyperemic PDV before banding when the vessel diameter was normal. The rationale for normalizing to PDV rather than to mean coronary velocity is that diastolic perfusion pressure is similar before and after banding (Li et al., 2003;Rockman et al., 1993) while systolic perfusion pressure is significantly elevated. The corrected baseline and hyperemic coronary velocities are shown in Fig. 6 with the raw values indicated by lines in each bar. The correction factors (1.4 to 1.7) shown at the bottom of each bar indicate increases of up to 30% in coronary artery diameter and correlate roughly to the pressure drops shown in Table 1 ($R^2 = 0.91$) suggesting that the cross-sectional area may increase in proportion to peak systolic pressure. This corrected figure shows a progressive increase in normalized baseline velocity and smaller increases in hyperemic velocity due to the increases in systolic coronary flow after banding, and suggests that the major cause for the reduction in H/B is an increase in baseline coronary flow as documented by others in man and in dogs (Eberli et al., 1989;Marcus et al., 1987;Parrish et al., 1985). We could not confirm an increase in coronary diameter post-mortem in the present study because the coronary arteries are not clearly visible on the surface of the heart, and the hearts of these mice were not perfusion-fixed to preserve the cross-section of vessels for histologic estimation of their diameters. However, because normalization affects both hyperemic and baseline velocities equally, CFR as estimated by the H/B ratio is unaffected by chronic coronary artery dilation.

Use of isoflurane as a coronary vasodilator

Anesthesia is required for most cardiovascular measurements in mice, and all known anesthetics alter cardiovascular function (Zuurbier et al., 2002; Jannsen et al., 2004). Isoflurane is known to slightly decrease peripheral vascular resistance, heart rate, and blood pressure such that these parameters may be slightly reduced at baseline. The baseline heart rates (393 to 446 b/min) at 1% isoflurane are similar to those recorded by telemetry from sleeping or resting mice (Kramer et al., 1999). The coronary vasodilator effects of isoflurane have been known for many years (Crystal et al., 1995; Crystal, 1996; Gamperi et al., 2002), but Kober et al. (2005) was the first to propose isoflurane as a noninvasive coronary vasodilator for estimating CFR in mice. The most common coronary vasodilator is adenosine (Hildick-Smith and Shapiro, 2000; Marcus, 1983) which produces a 4+ fold increase in coronary flow in humans (Hirata et al., 2001), although other investigators report smaller values (2.24) (Hozumi et al., 1998). Its use in mice has been problematic producing coronary flow increases on the order of 2.0 (Wikstrom et al., 2005) to 2.4 (Saraste et al., 2006). In our hands, adenosine given intravenously as a bolus to mice caused an initial bradycardic response followed by an increase in coronary

velocity of at most 2.2. In contrast, when the concentration of isoflurane is increased from 1% to 2.5%, a consistent hyperemic response occurs as shown in Fig. 1 with a similar peak diastolic velocity of 82–85 cm/s in young, adult, and old mice and with a minimal increase in heart rate averaging under 5% as shown in Fig. 4. Although isoflurane may not be a maximal coronary vasodilator (Gamperi et al., 2002), its use does not appear to underestimate CFR significantly. Indeed, our values for H/B (3.2) are slightly higher than CFR values reported by Wikstrom, et al. (2005) using adenosine (2.0) or hypoxia (1.9), by Saraste, et al. (2006) using adenosine (2.4), and even by Kober, et al. (2005) using isoflurane (2.4) in mice. The lower values reported by others in mice when compared to man and dogs have been attributed to the higher basal metabolism and lower cardiac reserve in smaller animals (Onozuka et al., 2002; Marcus, 1983). However, many investigators use isoflurane in concentrations exceeding 1% in mice (Wikstrom et al., 2005), and this could elevate the apparent baseline coronary flow or velocity and reduce the measured CFR. Our results support the findings of Kober, et al. (2005) and suggest that as a coronary vasodilator, isoflurane may be as effective as adenosine for applications in mice.

Increase in systolic coronary velocity

An unexpected observation was the significant increase in the systolic component of coronary flow as shown in Fig. 5 following aortic banding as the heart hypertrophied. A partial explanation is the large increase in systolic pressure generated by the band which is distal to the origin of the coronary arteries. However, the heart has to generate systolic pressure, and one would expect that the gradient between coronary arterial pressure and intramyocardial pressure during systole would remain low at least in the subendocardium. Indeed, when coronary flow is restricted to occur only during systole in dogs, there is relative under-perfusion of the subendocardium (Hess and Bache, 1976). In patients, we have observed similarly high systolic/diastolic velocity ratios in the right coronary arteries which supply mainly the right ventricle and both atria where the systolic compressive forces are lower (Cole and Hartley, 1977). Thus, the increase in the systolic component of coronary flow suggests a redistribution of perfusion toward the subepicardium. The S/D ratio is further increased during isoflurane-induced coronary vasodilation as shown in Fig. 5. Similarly high systolic velocities with an average S/D of 0.7 can been seen in the Doppler waveforms and data presented by Hozumi, et al. (1998) from the LAD coronary arteries of patients with aortic valve disease. Indeed, it has been found in patients and experimental animals that there is relative subendocardial under-perfusion and ischemia with pressure overload cardiac hypertrophy (Marcus, 1983;Hittinger et al., 1989;Hittinger et al., 1995), and subendocardial ischemia has been proposed as one of the precipitating factors leading to decompensated heart failure (Parrish et al., 1985;Vatner and Hittinger, 1993).

CONCLUSIONS

We show for the first time the serial and repeated measurement of coronary flow velocity in mice. The use of isoflurane gas at low and high concentrations as a coronary vasodilator when coupled with a method such as Doppler ultrasound to measure left main coronary flow or velocity provides a convenient and noninvasive method to estimate global coronary flow reserve in mice. Coronary flow reserve is reduced progressively and is virtually eliminated 21 days after transverse aortic banding due primarily to the increase in baseline myocardial work, energy consumption, and coronary flow. The large increase in the ratio of systolic/diastolic coronary velocity suggests a redistribution of perfusion from the endocardium to the epicardium as the heart remodels in response to pressure overload. The data presented show for the first time that the murine left ventricle and its coronary circulation respond similarly to those of man and dogs when the heart is subjected to chronic pressure overload. The reduction

in coronary reserve suggests a similar reduction in cardiac reserve which when exhausted is a prelude to decompensated heart failure.

Acknowledgments

The authors wish to acknowledge the contributions of Thuy Pham, Jennifer Pocius, and James Brooks for technical, surgical, and editorial assistance.

This work was supported in part by National Institutes of Health Grants R01-HL22512, P01-HL42550, R01-AG17899, R41-HL76928, and K25-HL73041.

REFERENCES

Bache RJ, Dai XZ, Alyono D, Vrobel TR, Homans DC. Myocardial blood flow during exercise in dogs with left ventricular hypertrophy produced by aortic banding and perinephritic hypertension. Circulation 1987;76:835–842. [PubMed: 2958173]

Barrick CJ, Rojas M, Schoonhoven R, Smyth SS, Threadgill DW. Cardiac response to pressure overload in 129Sl/SvImJ and C57BL/6J mice: temporal- and background-dependent development of concentric left ventricular hypertrophy. Am J Physiol Heart Circ Physiol 2007;292:H2119–H2130. [PubMed: 17172276]

Brickson S, Fitzsimons DP, Flack HA, Pereira L, Hacker T, Valdivia H, Moss RL. In vivo left ventricular function capacity is compromised in cMyBP-C null mice. Am J Physiol Heart Circ Physiol 2006;292:H1747–H1754. [PubMed: 17122190]

Cole JS, Hartley CJ. The pulsed Doppler coronary artery catheter: Preliminary report of a new technique for measuring rapid changes in coronary artery flow velocity in man. Circulation 1977;56:18–25. [PubMed: 862168]

Crystal GJ. Vasomotor effects of isoflurane in the coronary circulation. Anesthesiology 1996;84:1516–1517. [PubMed: 8669699]

Crystal GJ, Czinn EA, Silver JM, Ramez SM. Coronary vasodilation by isoflurane: Abrupt versus gradual administration. Anesthesiology 1995;82:542–549. [PubMed: 7856912]

Duncker DJ, Ishibashi Y, Bache RJ. Effect of treadmill exercise on transmural distribution of blood flow in hypertrophied left ventricle. Am J Physiol Heart Circ Physiol 1998;275:H1274–H1282.

Eberli FR, Ritter M, Schwitter J, Bortone A, Schneider J, Hess OM, Krayenbuehl HP. Coronary reserve in patients with aortic valve disease before and after successful aortic valve replacement. Eur Heart J 1989;12:127–138. [PubMed: 2044545]

Fallen EL, Elliott WC, Gorlin R. Mechanisms of angina in aortic stenosis. Circulation 1967;36:480–488. [PubMed: 6041860]

Gamperi AK, Hein TW, Kuo L, Cason BA. Isoflurane-induced dilation of porcine coronary microvesels is endothelium dependent and inhibited by glibenclamide. Anesthesiology 2002;96:1465–1471. [PubMed: 12170061]

Gould LK, Lipscomb K, Hamilton GW. Physiologic basis for assessing critical coronary stenosis: Instantaneous flow response and regional distribution during coronary hyperemia as measures of coronary flow reserve. Am J Cardiol 1974;33:87–94. [PubMed: 4808557]

Guyton JR, Hartley CJ. Flow restriction of one carotid artery in juvenile rats inhibits growth of arterial diameter. Am J Physiol Heart Circ Physiol 1985;248:H540–H546.

Hamawaki H, Coffman TM, Lashus A, Koide K, Zile MR, Oliverio MI, DeFreyte G, Cooper G IV, Carabello BA. Pressure-overload hypertrophy is unabated in mice devoid of AT_{1A} receptors. Am J Physiol Heart Circ Physiol 1998;274:H868–H873.

Hartley CJ, Reddy AK, Madala S, Martin-McNulty B, Vergona R, Sullivan ME, Halks-Miller M, Taffet GE, Michael LH, Entman ML, Wang YX. Hemodynamic changes in apolipoprotein E-knockout mice. Am J Physiol Heart Circ Physiol 2000;279:H2326–H2334. [PubMed: 11045969]

Hartley CJ, Reddy AK, Madala S, Michael LH, Entman ML, Taffet GE. Effects of isoflurane on coronary blood flow velocity in young, old, and ApoE−/− mice measured by Doppler ultrasound. Ultrasound in Med & Biol 2007;33:512–521. [PubMed: 17346873]

Hartley CJ, Taffet GE, Reddy AK, Entman ML, Michael LH. Noninvasive cardiovascular phenotyping in mice. ILAR Journal 2002;43:147–158. [PubMed: 12105382]

Hatle L, Brubakk A, Tromsdal A, Angelsen BAJ. Noninvasive assessment of pressure drop in mitral stenosis by Doppler ultrasound. Br Heart J 1978;40:131–140. [PubMed: 637964]

Hess DS, Bache RJ. Transmural distribution of myocardial blood flow during systole in the awake dog. Circ Res 1976;38:5–15. [PubMed: 1244228]

Hildick-Smith DJR, Shapiro LM. Coronary flow reserve improves after aortic valve replacement for aortic stenosis: An adenosine transthoracic echocardiographc study. J Am Coll Cardiol 2000;36:1889–1896. [PubMed: 11092661]

Hintze TH, Vatner SF. Reactive dilation of large coronary arteries in conscious dogs. Circ Res 1984;54:50–57. [PubMed: 6692499]

Hirata K, Shimada K, Watanabe H, Muro T, Yoshiyama M, Takeuchi K, Hozumi T, Yoshikawa J. Modulation of coronary flow velocity reserve by gender, menstrual cycle, and hormone replacement therapy. J Am Coll Cardiol 2001;38:1879–1884. [PubMed: 11738288]

Hittinger L, Mirsky I, Shen YT, Patrick TA, Bishop SP, Vatner SF. Hemodynamic mechanisms responsible for reduced subendocardial coronary reserve in dogs with severe left ventricular hypertrophy. Circulation 1995;92:978–986. [PubMed: 7641382]

Hittinger L, Shannon RP, Bishop SP, Geipi RJ, Vatner SF. Subendomyocardial exhaustion of blood flow reserve and increased fibrosis in conscious dogs with heart failure. Circ Res 1989;65:971–980. [PubMed: 2791231]

Hozumi T, Yoshida K, Akasaka T, Asami Y, Ogata Y, Takagi T, Kaji S, Kawamoto T, Ueda Y, Morioka S. Noninvasive assessment of coronary flow velocity and coronary flow velocity reserve in the left anterior descending coronary artery by Doppler echocardiography: Comparison with invasive technique. J Am Coll Cardiol 1998;32:1251–1259. [PubMed: 9809933]

Jannsen BJA, De Celle T, Debets JJM, Brouns AE, Callahan MF, Smith TL. Effects of anesthetics on systemic hemodynamics in mice. Am J Physiol Heart Circ Physiol 2004;287:H1618–H1624. [PubMed: 15155266]

Julius BK, Spillmann M, Vassalli G, Villari B, Eberli FR, Hess OM. Angina pectoris in patients with aortic stenosis and normal coronary arteries. Circulation 1997;95:892–898. [PubMed: 9054747]

Kober F, Iltis I, Cozzone PJ, Bernard M. Myocardial blood flow mapping in mice using high-resolution spin labeling magnetic resonance imaging: Influence of ketamine/xylazine and isoflurane anesthesia. Magn Reson Med 2005;53:601–606. [PubMed: 15723407]

Kramer K, Voss H, Grimbergen JA, Mills PA, Huetteman D, Zwiers L, Brockway B. Telemetric monitoring of blood pressure in freely moving mice: a preliminary study. Lab Animal 1999;34:272–280.

Li Y-H, Reddy AK, Taffet GE, Michael LH, Entman ML, Hartley CJ. Doppler evaluation of peripheral vascular adaptations to transverse aortic banding in mice. Ultrasound in Med & Biol 2003;29:1281–1289. [PubMed: 14553805]

Marcus, ML. The coronary circulation in health and disease. New York: McGraw-Hill; 1983.

Marcus ML, Doty DB, Hiratzka LF, Wright CB, Eastham CL. Decreased coronary reserve: a mechanism for angina pectoris in patients with aortic stenosis and normal coronary arteries. N Engl J Med 1982;307:1362–1366. [PubMed: 6215582]

Marcus ML, Harrison DG, Chillon J-M, Koyanagi S, Inou T, Tomanek RJ, Martins JB, Eastham CL, Hiratzka LF. Alterations in the coronary circulation in hypertrophied ventricles. Circulation 1987;75:119–125.

Maslov MY, Chacko VP, Stuber M, Moens AL, Kass DA, Champion HC, Weiss RG. Altered high-energy phosphate metabolism predicts contractile dysfunction and subsequent ventricular remodeling in pressure-overload hypertrophy mice. Am J Physiol Heart Circ Physiol 2007;292:H387–H391. [PubMed: 16963614]

Neishi Y, Akasaka T, Tsukiji M, Kume T, Wada N, Watanabe N, Kawamoto T, Kaji S, Yoshida K. Reduced coronary flow reserve in patients with congestive heart failure assessed by transthoracic Doppler echocardiography. J Am Soc Echocard 2005;18:15–19.

Niebauer J, Maxwell AJ, Lin PS, Tsao PS, Kosek J, Bernstein D, Cooke JP. Impaired aerobic capacity in hypercholesterolemic mice: partial reversal by exercise training. Am J Physiol Heart Circ Physiol 1999;276:H1346–H1354.

Onozuka H, Fujii S, Mikami T, Yamada S, Ishimori N, Shimizu T, Furumoto T, Nakai Y, Komuro K, Nishihara K, Okamoto H, Kitabatake A. In vivo echocardiographic detection of cardiovascular lesions in apolipoprotein E-knockout mice using a novel high-frequency high-speed echocardiography technique. Circ J 2002;66:272–276. [PubMed: 11922277]

Parrish DG, Ring WS, Bache RJ. Myocardial perfusion in compensated and failing hypertrophied left ventricle. Am J Physiol Heart Circ Physiol 1985;249:H534–H539.

Rockman HA, Knowlton KU, Ross J Jr, Chien KR. In vivo murine cardiac hypertrophy: a novel model to identify genetic signaling mechanisms that activate an adaptive physiological response. Circulation 1993;87:VII14–VII21.

Rushmer, RF. Cardiovascular Dynamics. Philadelphia: W.B. Saunders; 1976.

Sakata Y, Hoit BD, Ligget SB, Walsh RA, Dorn GW. Decompensation of pressure-overload hypertrophy in GaQ-overexpressing mice. Circulation 1998;97:1488–1495. [PubMed: 9576430]

Santagata P, Rigo F, Gherardi S, Pratali L, Drozdz J, Varga A, Picano E. Clinical and functional determinants of coronary flow reserve in non-ischemic dilated cardiomyopathy: An echocardiographic study. Int J Cardiol 2005;105:46–52. [PubMed: 16207544]

Saraste A, Kyto V, Saraste M, Vuorinen T, Hartiala J, Saukko P. Coronary flow reserve and heart failure in experimental coxsackievirus myocarditis. A transthoracic Doppler echocardiography study. Am J Physiol Heart Circ Physiol 2006;291:H871–H875. [PubMed: 16501009]

Saraste M, Koskenvuo JW, Knuuti J, Toikka JO, Laine H, Niemi P, Sakuma H, Hartiala JJ. Coronary flow reserve: measurement with transthoracic Doppler echocardiography is reproducible and comparable with positron emission tomography. Clin Physiol 2001;21:114–122. [PubMed: 11168305]

Tanaka N, Dalton N, Mao L, Rockman HA, Peterson KL, Gottshall KR, Hunter JJ, Chien KR, Ross J. Transthoracic echocardiography in models of cardiac disease in the mouse. Circulation 1996;94:1109–1117. [PubMed: 8790053]

Vatner SF, Hittinger L. Coronary vascular mechanisms involved in decompensation from hypertrophy to heart failure. J Am Coll Cardiol 1993;22:34A–40A.

White CW, Wright CB, Doty DB, Hiratza LF, Eastham CL, Harrison DG, Marcus ML. Does visual interpretation of the coronary arteriogram predict the physiological importance of a coronary stenosis? N Engl J Med 1984;310:819–824. [PubMed: 6700670]

Wikstrom J, Gronros J, Bergstrom G, Gan LM. Functional and morphologic imaging of coronary atherosclerosis in living mice using high-resolution color Doppler echocardiography and ultrasound biomicroscopy. J A C C 2005;46:720–727.

Zhang Y-M, Bo J, Taffet GE, Chang J, Shi J, Reddy AK, Michael LH, Schneider MD, Entman ML, Schwartz RJ, Wei L. Targeted deletion of ROCK1 protects the heart against pressure overload by inhibiting reactive fibrosis. FASEB J 2006;20:916–925. [PubMed: 16675849]

Zuurbier CJ, Emons VM, Ince C. Hemodynamics of anesthetized ventilated mouse models: aspects of anesthetics, fluid support, and strain. Am J Physiol Heart Circ Physiol 2002;282:H2099–H2105. [PubMed: 12003817]

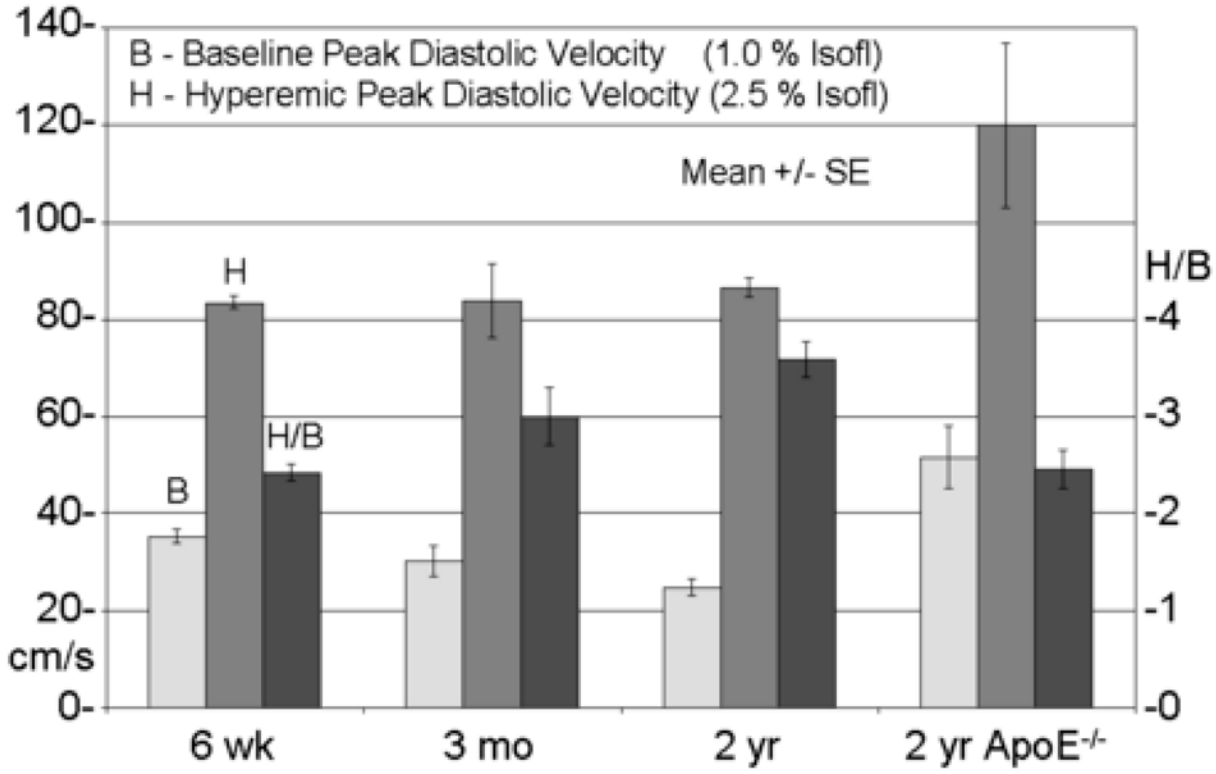

Fig. 1.

Baseline (B) and hyperemic (H) peak diastolic coronary velocity and H/B ratio in 10 6-week, 10 3-month, and 10 2-year-old mice and in 20 2-year-old apolipoprotein-E null ($ApoE^{-/-}$) mice.

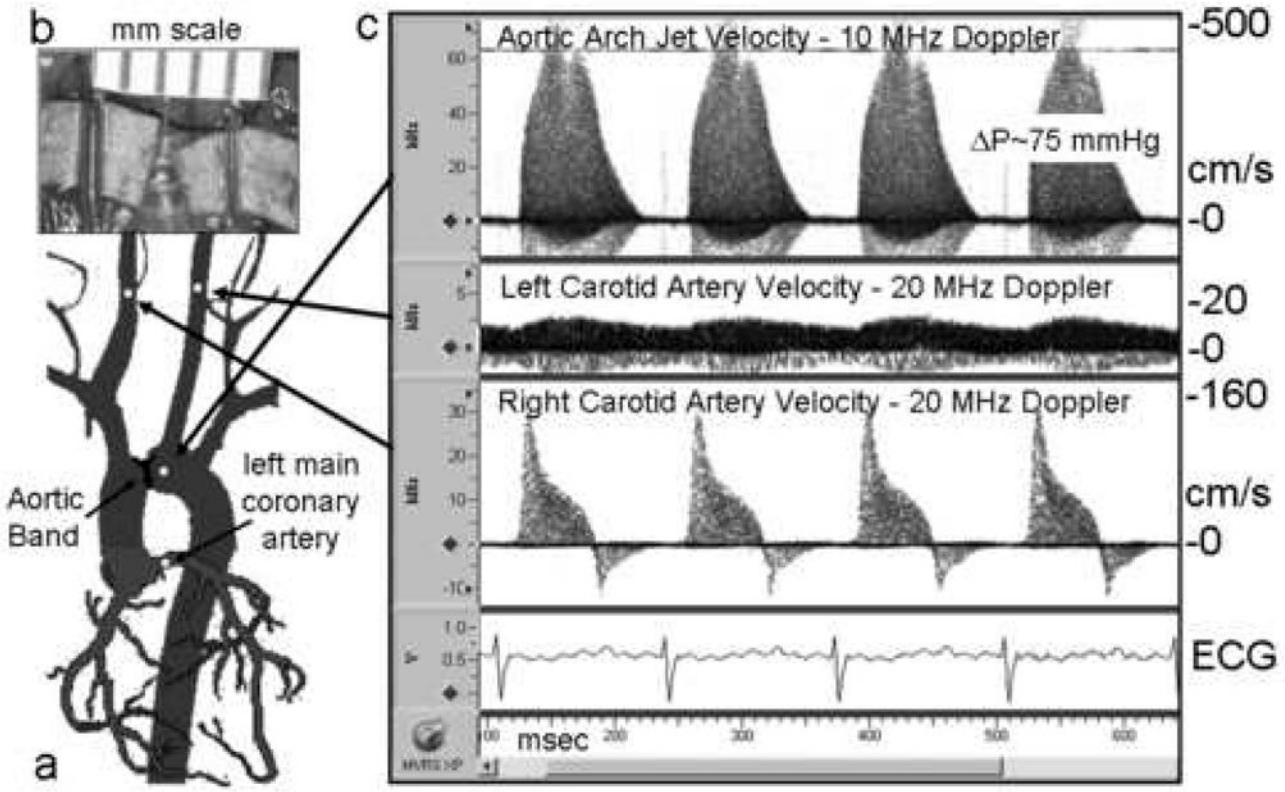

Fig. 2.

Diagram showing the location of the transverse aortic band (a), photograph of the right and left carotid arteries 2 weeks after banding (b), and a display of Doppler spectral signals from the location of the band, the left carotid artery, and the right carotid artery three weeks after banding (c).

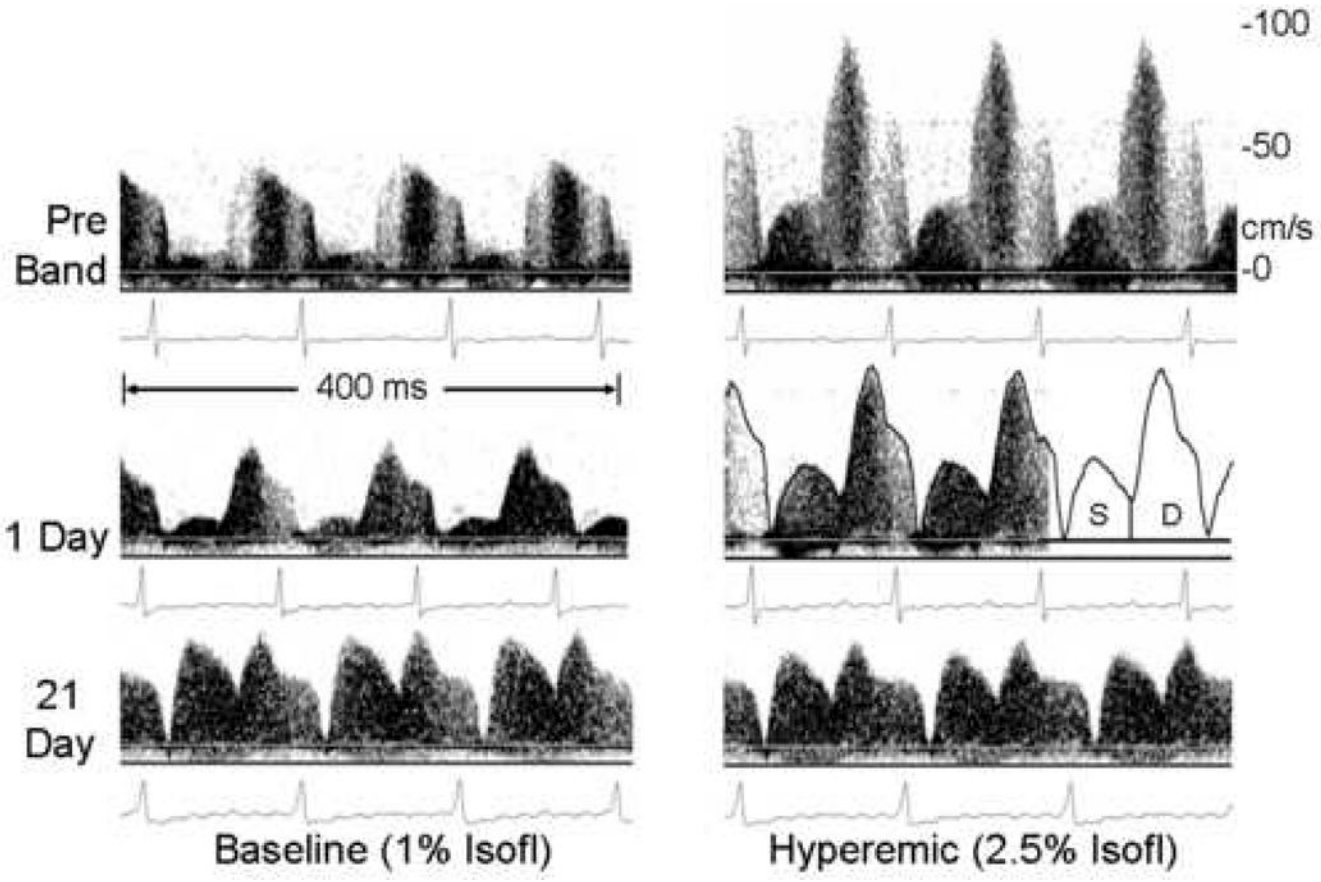

Fig. 3.

Doppler signals taken from the left coronary artery of a mouse before banding (Pre-Band) and 1 and 21 days after banding at low (1%) and high (2.5%) concentrations of isoflurane gas anesthesia. A spectral envelope calculated by the software is shown on the 1 day hyperemic display illustrating how systolic (S) and diastolic (D) time-velocity areas used in calculating S/D ratios are determined.

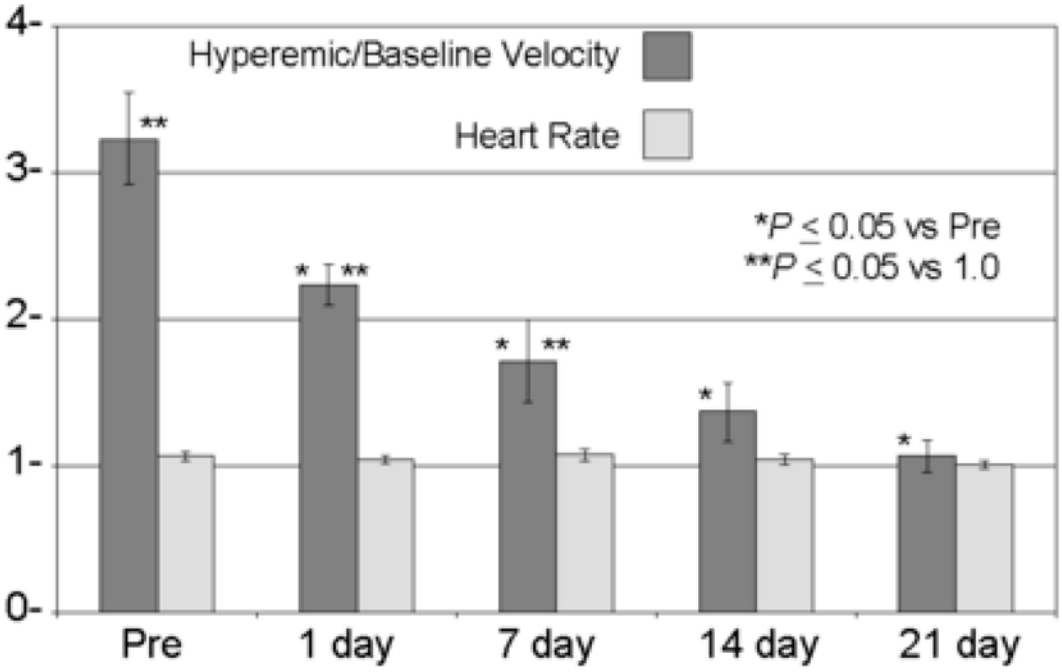

Fig. 4.

Ratio of hyperemic/baseline velocity and heart rate at the five time points. The increase in velocity at hyperemia versus baseline is significantly different from 1.0 (no increase) Pre and at 1 and 7 days, and is significantly different from Pre at all time points. The increase in heart rate at hyperemia versus baseline is not statistically significant at any time point.

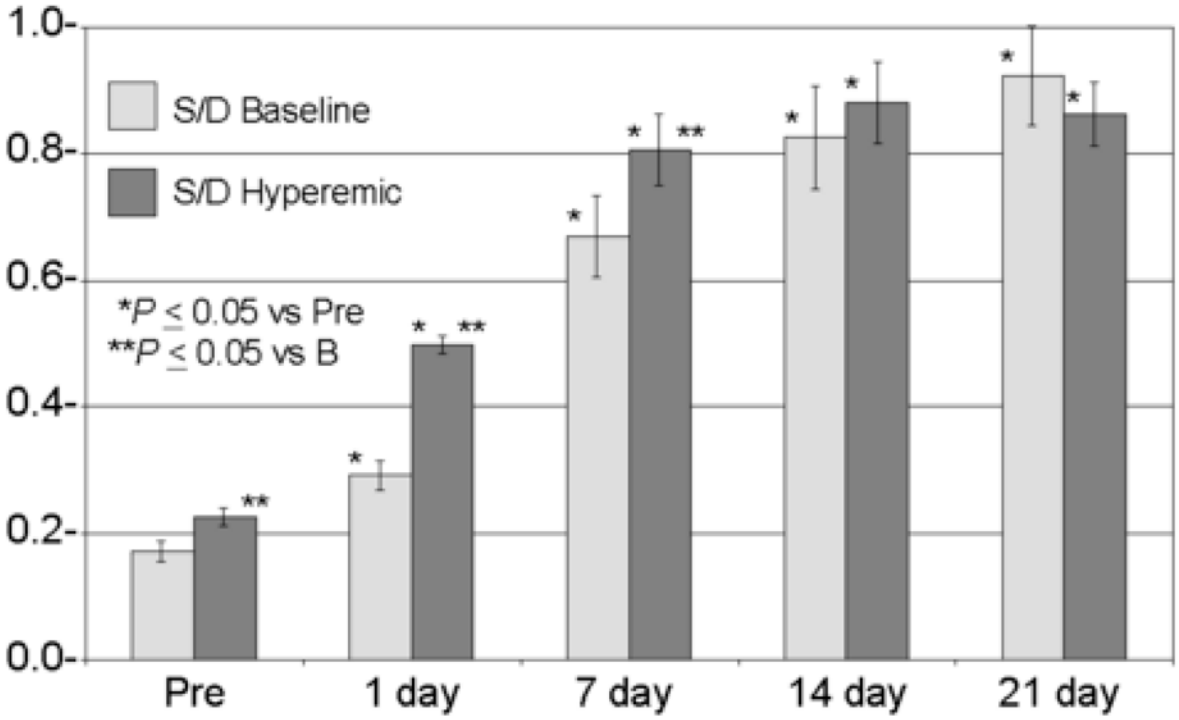

Fig. 5.

Systolic/diastolic area ratios (S/D) at baseline and hyperemia at the five time points. The S/D ratio is statistically different after banding at both baseline and hyperemia at all time points, and the increase in S/D from baseline to hyperemia is significant before and at 1 and 7 days after banding.

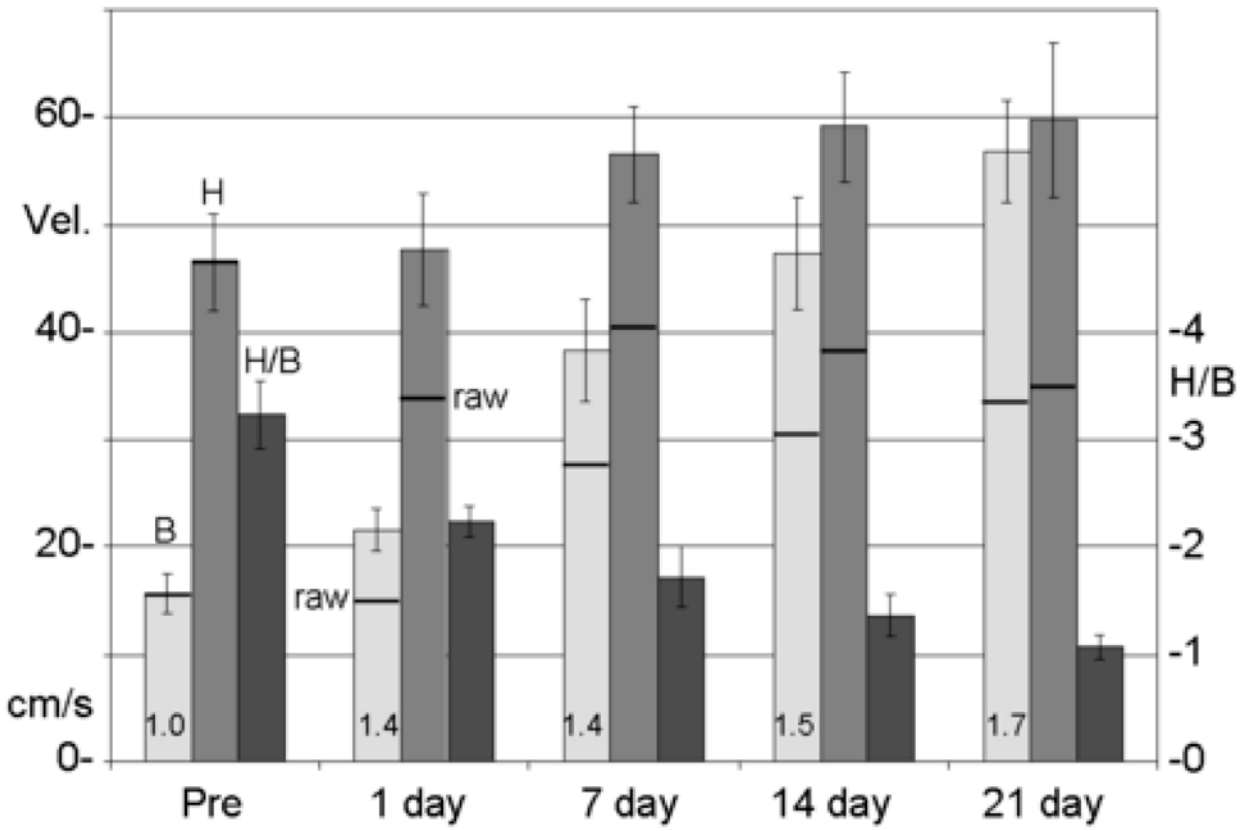

Fig. 6.

Baseline velocity (B), hyperemic velocity (H), and H/B at all time points normalized to hyperemic peak diastolic velocity (PDV) to account for pressure-induced dilation of the coronary artery. The raw values for B and H are shown by lines in each bar. The graph should closely represent changes related to coronary volume flow rather than velocity. The normalizing factors are shown at the bottom of each set of bars.

Table 1

Summary of data from 10 mice before and after aortic banding

Parameter		Units	Pre band	1-day	7-day	14-day	21-day
Number		n	10	10	9	9	8
Aortic Vel	Mean	cm/s	19.5 ± 1.7	18.5 ± 1.5	20.7 ± 1.6	18.5 ± 1.9	21.5 ± 1.7
Mitral Vel	Mean	cm/s	14.3 ± 1.1	11.5 ± 1.3	13.4 ± 1.1	13.2 ± 1.4	14.9 ± 1.6
R Carotid	Max	cm/s	37.7 ± 2.4	73.0 ± 4.5 *	81.9 ± 5.4 *	87.9 ± 5.7 *	82.7 ± 6.2 *
	Min	cm/s	1.6 ± 0.8	−10.9 ± 2.4 *	−19.1 ± 2.1 *	−20.3 ± 2.3 *	−19.1 ± 1.7 *
	Mean	cm/s	11.1 ± 0.6	11.4 ± 1.3	12.5 ± 0.7	15.9 ± 1.1	15.2 ± 1.0
	PI	ratio	3.24 ± 0.15	9.02 ± 1.99 *	8.13 ± 0.42 *	7.62 ± 0.98 *	6.72 ± 0.30 *
L Carotid	Max	cm/s	38.9 ± 2.7	9.8 ± 0.8 *	12.6 ± 1.0 *	11.6 ± 1.1 *	8.3 ± 0.9 *
	Min	cm/s	3.5 ± 0.4	5.3 ± 0.9	1.6 ± 0.5	5.5 ± 1.0	3.3 ± 0.8
	Mean	cm/s	12.1 ± 0.7	7.2 ± 0.7	8.0 ± 0.9	8.7 ± 1.1	6.1 ± 0.8
	PI	ratio	2.92 ± 0.09	0.74 ± 0.15 *	1.55 ± 0.22 *	0.78 ± 0.11 *	0.88 ± 0.08 *
R/L Carot	Max	ratio	0.97 ± 0.06	7.45 ± 0.45 *	6.50 ± 0.43 *	7.58 ± 0.49 *	9.96 ± 0.75 *
	Mean	ratio	0.92 ± 0.05	1.58 ± 0.16 *	1.56 ± 0.09 *	1.83 ± 0.13 *	2.49 ± 0.17 *
	PI	ratio	1.11 ± 0.06	12.32 ± 2.73 *	5.25 ± 0.75 *	9.77 ± 1.24 *	7.64 ± 0.69 *
Jet Vel	Peak	cm/s	73 ± 4.02	352 ± 17.39 *	390 ± 20.51 *	407 ± 12.23 *	426 ± 16.48 *
D Pressure	4V2^	mmHg	2.2 ± 0.24	51 ± 5.14 *	62 ± 6.10 *	67 ± 4.05 *	74 ± 5.15 *
Baseline							
HR		b/min	393 ± 20	396 ± 19	427 ± 19	446 ± 20	414 ± 18
Coron Vel	Mean	cm/s	15.6 ± 1.8	15.3 ± 1.4	27.5 ± 3.4 *	30.6 ± 3.4 *	33.2 ± 2.8 *
Coron Vel	PDV	cm/s	30.1 ± 3.1	30.5 ± 2.4	44.6 ± 4.3 *	44.0 ± 3.7 *	46.8 ± 4.0 *
S/D		ratio	0.17 ± 0.02	0.29 ± 0.02 *	0.67 ± 0.06 *	0.83 ± 0.08 *	0.92 ± 0.08 *
Hyperemic							
HR		b/min	415 ± 15	408 ± 17	452 ± 14	457 ± 12	415 ± 16
Coron Vel	Mean	cm/s	46.5 ± 4.5 **	33.8 ± 3.7 **	40.6 ± 3.2	38.1 ± 3.3	34.9 ± 4.2
Coron Vel	PDV	cm/s	83.9 ± 7.5 **	59.5 ± 6.7 **	60.3 ± 3.7	54.0 ± 4.6	49.2 ± 6.2
S/D		ratio	0.23 ± 0.01	0.50 ± 0.01 *	0.81 ± 0.06 *	0.88 ± 0.06 *	0.86 ± 0.05 *
H/B							
HR		ratio	1.07 ± 0.03	1.04 ± 0.03	1.07 ± 0.04	1.04 ± 0.04	1.01 ± 0.03
Coronary	Mean	ratio	3.23 ± 0.32	2.24 ± 0.14 *	1.72 ± 0.28 *	1.37 ± 0.20 *	1.06 ± 0.11 *
Coronary	PVD	ratio	2.97 ± 0.26	1.95 ± 0.11 *	1.52 ± 0.23 *	1.28 ± 0.15 *	1.05 ± 0.08 *
Body Wt		g	22.20 ± 0.70	22.08 ± 0.60	21.20 ± 0.70	21.80 ± 0.50	22.25 ± 0.52
Heart Wt		mg					183 ± 6.29
HW/BW		mg/g	5.77 ± 0.25 ^		6.70 ± 0.25 ^		8.30 ± 0.43

* P < 0.05 versus Pre

** P < 0.05 versus baseline

^ Data from previous studies for reference

All data are mean ± SE, Vel - velocity, R - right, L - left, HR - heart rate, S/D - systolic/diastolic time-velocity area, H/B - hyperemic/baseline, Wt - weight, HW/BW - heart weight/body weight